

LA-UR-79-2849

MASTER  
MAILED

**TITLE:** HIGH-RESOLUTION FISSION CROSS SECTION OF  $^{231}\text{Pa}$

**AUTHOR(S):** S. Plattard, G. F. Auchampaugh, N. W. Hill,  
G. de Saussure, R. B. Perez and J. A. Harvey

**SUBMITTED TO:** International Conference on Nuclear Cross  
Sections for Technology, October 22-26, 1979

By acceptance of this article, the publisher recognizes that the U.S. Government retains a non-exclusive, royalty-free license to publish or reproduce the published form of this contribution, or to authorize others to do so, for U.S. Government purposes.

The Los Alamos Scientific Laboratory requests that the publisher identify this article as work performed under the auspices of the Department of Energy.



**los alamos**  
**scientific laboratory**  
of the University of California  
LOS ALAMOS, NEW MEXICO 87545

An Affirmative Action/Equal Opportunity Employer

## HIGH-RESOLUTION FISSION CROSS SECTION OF $^{231}\text{Pa}$ \*

S. Plattard,<sup>†</sup> G. F. Auchampaugh  
University of California, Los Alamos Scientific Laboratory  
Los Alamos, New Mexico 87545 USA

N. W. Hill, G. de Saussure, R. B. Perez and J. A. Harvey  
Oak Ridge National Laboratory  
Oak Ridge, Tennessee 37830 USA

A high-resolution fission cross section for  $^{231}\text{Pa}$  was measured at ORELA from 0.1 to 12 MeV and between 0.4 eV and 10 keV. The data show evidence for 1) fractionated vibrational structures in the threshold region of the fission cross section, and 2) narrow fission resonances above 1.5 eV with an average fission width  $\langle \Gamma_f \rangle = 8 \text{ eV}$ .

[ $^{231}\text{Pa}(n,f)$  cross section 0.4 eV - 10 keV and 0.1 - 12 MeV, measured  $\Gamma_f$  below 60 eV.]

### Introduction

Previous measurements of the  $^{231}\text{Pa}(n,f)$  cross section above 100 keV<sup>1,2</sup> show considerable structure in the threshold region of the fission cross section. These structures have been interpreted<sup>2</sup> as vibrational states of known spin and parity trapped in the second minimum of the double-humped fission barrier of  $^{232}\text{Pa}$ . However, since these resonances occur at rather high excitation energy, they may be fragmented into more complex states. To investigate such a possibility, we have undertaken at ORELA a high-resolution fission cross section measurement of  $^{231}\text{Pa}$ .

\*Work supported in part by the U.S. Department of Energy.

<sup>†</sup>Permanent address: Centre d'Etudes de Bruyères-le-Château, BP561, 92542 Montrouge Cedex, France.

Taking advantage of the high chemical purity of the  $^{231}\text{Pa}$  samples (less than 0.1 ppm of fissile elements) a preliminary measurement in the eV region was also carried out. For the first time, narrow fission resonances were observed above 1.3 eV.

Besides the importance of  $^{231}\text{Pa}$  for basic fission studies, it is also of interest in the field of reactor design in that it plays a part in the unwanted generation of  $^{232}\text{U}$  in the  $^{232}\text{Th}/^{233}\text{U}$  breeder cycle.

#### Experimental Procedure

The  $^{231}\text{Pa}(n,f)$  cross section  $\sigma_f$  relative to the  $^{235}\text{U}$  fission cross section was measured using neutrons produced by the Oak Ridge Electron Linear Accelerator (ORFEL) used as a pulsed source. Fission fragments were detected by a gas scintillator located on a flight path perpendicular to the electron beam. Table I summarizes the experimental conditions for both the high energy [ $0.1 < E_n(\text{MeV}) \leq 12$ ] and the low energy [ $0 < E_n(\text{keV}) < 10$ ] measurements.

Table I. Experimental Conditions

	$0.1 < E_n(\text{MeV}) \leq 12$	$0 < E_n(\text{keV}) < 10$
Frequency (Hz)	800	450
Pulse width (ns)	6 - 8	40
Power (kW)	8 - 9	26
Average flight path (m)	41.68	18.30
Filters	none	0.5 mm of Cd.
Duration (h)	632	60

The fission detector consisted of a sealed cylindrical chamber containing a mixture of 98% He and 2%  $N_2$  at STP. The chamber was divided into 3 pairs of optically isolated cells. The distance between two consecutive pairs was 12.5 cm. Each cell was viewed through two circular quartz windows by two XP2020/Q photomultiplier tubes.

Each of the five  $^{231}\text{Pa}$  cells contained 53 mg of protactinium oxide painted on both sides of a semicircular titanium foil (20 cm in diameter and 12.5  $\mu\text{m}$  thick) to a density of approximately  $0.3 \text{ mg/cm}^2$ . The remaining cell contained 140 mg of uranium enriched to 93% in  $^{235}\text{U}$ . The uranium was electroplated on both sides of a semicircular stainless-steel disk (250  $\mu\text{m}$  thick) to a density of  $0.5 \text{ mg/cm}^2$ .

To define a valid fission event and to reduce alpha background and noise we require a coincidence between the pair of photomultiplier tubes on each cell. The fission events from each cell once digitized and routed by an EG&G TDC 100 clock were stored separately in the computer. Both pulse-height and time-of-flight information were recorded to provide a continuous monitor as a function of neutron energy of the fission bias for each cell.

#### Data Reduction

$E_n > 0.1 \text{ MeV}$ . After background corrections, which were assumed essentially constant for the  $^{231}\text{Pa}$  and  $^{235}\text{U}$  time-of-flight (TOF) spectra, the shape of the  $^{231}\text{Pa}(n,f)$  cross section was obtained using the  $^{235}\text{U}(n,f)$  cross section derived from ENDF/B-V. The  $^{231}\text{Pa}$  fission cross section was normalized between 0.9 and 1.1 MeV to the data of Sicre<sup>2</sup>. In this procedure it was assumed implicitly that the efficiency of the detector was independent of neutron energy.

$E_n < 10$  keV. Since the data recorded in this energy region can provide only preliminary results, due to the limited available beam time for this measurement, the simplest possible reduction procedure was adopted. By assuming that the energy dependence of the neutron flux is close to  $1/E_n$ ,  $\sigma_f \sqrt{E_n}$  is proportional to the  $^{231}\text{Pa}$  TOF spectrum. The proportionality constant was determined by the ratios of  $^{231}\text{Pa}/^{235}\text{U}$  counts at 230 and 380 keV and from the known fission cross section at 13.26 eV for  $^{235}\text{U}$ . As a check of the energy dependence of the neutron flux, the  $^{235}\text{U}$  TOF spectrum was compared to  $\sigma_f^{235}\sqrt{E_n}$ . The two sets of data agree to within a few percent between 0.4 and 100 eV.

#### Results

The  $^{231}\text{Pa}(n,f)$  cross section is plotted in Fig. 1 from 0.1 to 12 MeV. The peaks and the strong fluctuations observed below 1 MeV are superimposed on an underlying cross-section characteristic of a neutron-induced threshold fission reaction whose threshold is located around 750 keV. The second chance fission threshold occurs in the vicinity of  $E_n = 6$  MeV leading to a plateau value for  $\sigma_f$  of  $\sim 2$  b.

Figure 2 displays a more detailed picture of  $\sigma_f$  between 0.12 and 0.42 MeV. For comparison we have plotted the data of Sicre<sup>2</sup> which were taken with a resolution of 5 keV, except for the 160-keV data point which was taken with a resolution of 2 keV. The Sicre data are systematically lower even though the present data were normalized to his cross section in the 0.9- to 1.1-MeV region. The striking feature of this figure lies in the considerable amount of fine structure in the cross section which has not been observed in previous measurements. This is due to the substantial improvement in the resolution of the present measurement. For instance, at 160 keV our resolution is 0.4 keV. As a result, the resonance at 156.7

keV which has a FWHM of 2.9 keV is now completely resolved. However, the base of this resonance cannot be described by the wings of a Breit-Wigner function. This suggests the presence of additional structure centered around the 157-keV peak. In addition, the good energy resolution reveals the presence of other sharp resonances (at least two in the vicinity of  $E_n = 370$  keV) and separates into several components the broad peaks located around  $E_n = 180$  and 330 keV. Table II gives a preliminary list of the peak energies of  $\sigma_f$  together with  $K^\pi$  values extracted from ref. 2.

TABLE II: Resonance Energies and Corresponding  $K^\pi$  Values

<u><math>E_n</math>(keV)</u>	<u><math>K^\pi</math></u>	<u><math>E_n</math>(keV)</u>	<u><math>K^\pi</math></u>
156.7	$3^+$	304.5	
173.3		312.1	
182.3		319.5	
187.4		328.6	$0^-$
193.8	$0^+$	336.7	
281.9		371.2	
300.6		375.7	

Below 100 eV (see Fig. 3), a number of fission resonances are observed for the first time except for the 4 resonances below 1.3 eV already reported by Leonard et al.<sup>3</sup> The resonance energies are in very good agreement with those given by Simpson et al.<sup>4</sup> in their total cross-section measurement. However, we observe additional resonances

above 15 eV. Rather than being clustered around definite energies as it has been observed in several subthreshold cross sections,<sup>5-8</sup> these resonances seem to be uniformly distributed, at least below 100 eV. Because of poor statistics at higher energies, it is not possible at the present time to verify if this behavior is also valid in the keV region. From the  $g\Gamma_n$  values reported in ref. 9, the  $\Gamma_f$  values have been calculated and are listed in Table III together with other resonance parameters. A meaningful average fission width  $\langle \Gamma_f \rangle$  can be obtained only for those resonances below 15 eV because resonances were missed above this energy in the total cross section measurement. The average fission width for those resonances below 15 eV is 8  $\mu$ eV, about 3 to 4 orders of magnitude lower than what is generally measured for fissile nuclei. In the energy region analyzed,  $[1.24 < E_n(\text{eV}) < 57.3]$  no significant enhancement of  $\Gamma_f$  is noted. This is similar to the behavior of the fission widths for the fissile nuclei.

#### Discussion

Sicre<sup>2</sup> concludes from his fission fragment angular distribution measurements on  $^{231}\text{Pa}$  that the resonance at 156.7 keV is a pure vibrational state having  $K^\pi = 3^+$ . However, our data suggest that this resonance is fragmented. A possible explanation for this fragmentation may be due to a rotational band built on this vibrational state. The resonances of this band would have  $J^\pi > 3^+$  and therefore be formed with  $l \geq 3$  neutrons leading to peak cross sections on the order of a few mb. This is consistent with the magnitude of the structure observed in the tails of the 156.7-keV peak. However, the spacing of members of such a rotational band is on the order of 20 keV if we assume  $\hbar^2/2I \approx 2$  to

3 keV as reported for  $^{240}\text{Pu}^{10}$  and  $^{231,233}\text{Th}^{11,12}$ . This spacing is much larger than the energy span of the underlying structure. A spacing of a few keV would require a moment of inertia  $\mathcal{I}$  incompatible with a stable shape of the nucleus.

To interpret the particular shape of this resonance we propose the following picture in the framework of the calculations of Möller et al.<sup>13,14</sup> This resonance could represent a vibrational state trapped in the shallow asymmetrically deformed third minimum of the triple-humped fission barrier of  $^{232}\text{Pa}$ . The additional observed structure would come from coupling between this vibrational state (Class-III state) and several less deformed and more complex states (Class II states) that exhibit an average spacing  $\langle D_{II} \rangle$  of a few keV. The gross structures observed by Sicre<sup>2</sup> at approximately 180 and 330 keV were interpreted in terms of  $K^\pi = 0^+$  and  $0^-$  rotational band respectively. We observe more structure than can be accounted for by just two simple rotational bands. As in the case of the 156.7-keV resonance, this additional structure may be due to the fragmentation of the members of the rotational bands.

Since we adopt the model of an asymmetrically deformed third minimum, one should expect to find vibrational states of both parities as it can be verified by a WKB calculation.<sup>15</sup> We speculate that the resonance located at 173.3 keV could be a possible candidate for a  $K^\pi = 3^-$  vibrational state. Indeed, 1) the peak cross section has the correct magnitude to be formed with  $l = 2$  neutrons and 2) its separation from the  $3^+$  state (16.6 keV below) is comparable to what has been reported by Blons et al.<sup>12</sup> for  $^{231}\text{Th}$  and calculated by Möller et al.<sup>14</sup> for this mass region.

We also would like to point out that the fission widths of the narrow resonances observed in the eV region are consistent with the shape of the barrier calculated by Möller and Howard<sup>14</sup> for  $^{232}\text{Pa}$ . Including axial asymmetry (gamma deformation) in their calculations lowers the first maximum below the neutron separation energy  $S_n$  in  $^{232}\text{Pa}$ . In addition, since the third minimum is shallow and the neutron-induced fission threshold is  $\sim 750$  keV above  $S_n$ , a nucleus undergoing fission in the eV region only will be sensitive to the overall shape of the outer two barriers. If we approximate the shape of the outer barriers by a simple parabola with curvature  $\hbar\omega$  then we calculated an  $\hbar\omega = 0.5$  MeV when using 8  $\mu\text{eV}$  for the average fission width  $\langle\Gamma_f\rangle$ . This value of the curvature for the outer barrier is in fairly good agreement with that reported by Back *et al.*<sup>16</sup> for odd-odd actinides.

#### Conclusion

This measurement has revealed a considerable amount of fine structure in the threshold region of the neutron-induced fission cross section of  $^{231}\text{Pa}$ . We speculate that some of the newly observed structure may be due to coupling between vibrational states of the third well to more complex states of the second well of the fission barrier. A more accurate knowledge of the fission mechanism for this nucleus would require a high-resolution measurement of 1) the fission fragment anisotropies between 0.1 and 0.4 MeV and 2) the fission cross section in the keV region to look for possible intermediate structure. In addition, other experiments such as study of the  $\gamma$  rays emitted from the  $^{231}\text{Pa}(d,p\gamma)$  reaction below  $S_n$  would provide a sensitive probe for determining the depth of the first and the second minima of the fission barrier.

Acknowledgments

We are particularly indebted to P. Möller and M. Howard for fruitful discussions and access to their recent results prior to publication. We are grateful to P. Kuehn from the Solid State Division of Oak Ridge National Laboratory for the very successful preparation of the  $^{231}\text{Pa}$  samples. The staff of ORELA should also be thanked for the smooth operation of the Linac. One of us (S. P.) would like specially to thank the Physics Division of the Los Alamos Scientific Laboratory for its warm hospitality and constant support during this experiment.

References

1. D. W. Muir and L. R. Veaser, in Proceedings of the Conference on Nuclear Cross Sections and Technology, Knoxville, TN, March 15-17, 1971, p. 292.
2. A Sicre, thesis, University of Bordeaux (1976), Report CENBG 7603.
3. B. R. Leonard, Jr., and R. H. Odegaarden, Bull. Amer. Phys. Soc., 6, 8 (1961); Hanford Report 67219 (1960).
4. F. B. Simpson, W. H. Burgus, J. E. Evans and H. W. Kirby, Nucl. Sci. Eng., 12, 243 (1960).
5. D. Paya, H. Derrien, A. Fubini, A. Michaudon and P. Ribon, in Nuclear Data for Reactors, IAEA Vienna 1967, II, p. 128; A. Fubini, J. Blons, A. Michaudon and D. Paya, Phys. Rev. Lett., 20, 1373 (1968).
6. E. Migneco and J. P. Theobald, Nucl. Phys., A112, 603 (1968).
7. G. D. James, J. T. Dabbs, J. A. Harvey, N. W. Hill and R. H. Schindler, Phys. Rev., C15, 2083 (1977).
8. F. C. Difilippo, R. B. Perez, G. de Saussure, D. K. Olsen, R. W. Ingle, Nucl. Sci. Eng., 68, 43 (1978).
9. BNL 325, 1, Third Edition (1973).
10. H. J. Specht, J. Weber, F. Konecny and D. Heunemann, Phys. Lett., 41B, 43 (1972).
11. J. Blons, C. Mazur and D. Paya, Phys. Rev. Lett., 35, 1749 (1975).
12. J. Blons, C. Mazur, D. Paya, M. Ribrag and H. Weigmann, Phys. Rev. Lett., 41, 1282 (1978).
13. P. Möller and J. R. Nix, in Proceedings of Physics and Chemistry of Fission, IAEA Vienna 1974, I p. 103.
14. P. Möller and M. Howard, private communication (1979).

15. L. D. Landau and E. M. Lifshitz, in Quantum Mechanics, Pergamon Press (1958), p. 176.
16. B. B. Back, J. P. Bondorf, G. A. Ostroschenko, J. Pedersen and B. Rasmusen, Nucl. Phys., A165, 449 (1971).

TABLE III. FISSION WIDTHS AND OTHER ASSOCIATE PARAMETERS FROM 1 eV to 55 eV FOR  $^{235}\text{Pu} + n$ .

$E_n$ (eV)	$A_f$ (b-eV)	$g\Gamma_n$ (meV)	$l$ (m-d)	$\Gamma_f$ ( $\mu$ eV)	$E_n$ (eV)	$A_f$ (b-eV)	$g\Gamma_n$ (meV)	$l$ (m-d)	$\Gamma_f$ ( $\mu$ eV)
1.24	0.0079	0.0280	46	8	22.12	0.0134	0.4700	50	34
1.40	0.0	0.0032	45	0	24.75	0.0125	0.2790	50	24
1.96	0.0014	0.0071	46	9	25.45	0.0037	0.0930	50	29
2.79	0.0029	0.0099	39	16	27.97	0.0364	1.0790	50	3
3.48	0.0108	0.0470	44	19	28.85	0.0027	0.1550	50	3
4.12	0.0043	0.0850	50	5	27.32	0.0258	0.4440	50	24
4.35	0.0020	0.0600	60	4	28.23	0.0033	0.2020	50	23
4.53	0.0013	0.0170	55	9	28.69	0.0044	0.2680	50	10
5.06	0.0070	0.4900	63	2	29.62	0.0046	1.6870	50	7
5.20	0.0017	0.0850	45	2	30.22	0.0033	0.0550	50	45
5.63	0.0016	0.0470	45	4	31.73	0.0332	3.3800	50	3
5.82	0.0049	0.0580	45	11	32.20	0.0010	0.0570	50	30
6.55	0.0014	0.0490	50	5	32.80	0.0046	0.1800	50	10
6.87	0.0076	0.2500	46	5	33.39	0.0017	0.1490	50	30
7.57	0.0058	0.0930	60	14	34.15	0.0043	0.2000	50	19
7.57	0.0092	0.1820	55	11	36.14	0.0035	0.3900	50	5
8.73	0.0142	0.7400	57	5	36.65	0.0025	1.4590	50	3
9.26	0.0006	0.0460	55	3	36.80	0.0033	0.3690	50	3
9.70	0.0073	0.2300	50	8	37.53	0.0119	0.9990	50	3
10.33	0.0461	0.7000	49	16	38.26	0.0000	0.2000	50	3
10.76	0.0071	0.3410	30	3	39.73	0.0077	1.0500	50	3
11.26	0.0101	0.3620	50	2	41.27	0.0055	0.6500	50	10
11.67	0.0199	0.6830	50	8	42.08	0.0145	0.6500	50	10
12.08	0.0005	0.0216	50	8	43.34	0.0092	1.4100	50	3
13.26	0.0331	0.8010	50	13	44.54	0.0009	0.1000	50	3
13.38	0.0345	1.0970	50	10	44.91	0.0023	0.1150	50	10
14.10	0.0029	0.5780	50	2	45.64	0.0144	1.2200	50	3
15.06	0.0043	0.1090	50	15	46.39	0.0075	0.3350	50	10
15.57	0.0112	0.2010	50	21	47.22	0.0022	1.0300	50	3
16.02	0.0059	0.3280	50	7	48.60	0.0043	0.2920	50	3
16.66	0.0043	0.2290	50	8	50.12	0.0030	0.1300	50	10
16.99	0.0055	0.3060	50	7	50.85	0.0209	0.8500	50	3
18.29	0.0103	1.5140	50	3	51.25	0.0000	0.4900	50	3
18.74	0.0195	0.6930	50	13	51.42	0.0115	0.0500	50	3
19.25	0.0036	0.1760	50	10	52.54	0.0105	2.1500	50	3
19.55	0.0013	0.0800	50	8	53.91	0.0122	0.8000	50	3
20.30	0.0016	0.0410	50	19	54.44	0.0117	1.3600	50	3
20.60	0.0003	0.9990	50	10	55.20	0.0000	4.2000	50	3
21.30	0.0056	0.5540	50	5	56.52	0.0000	0.8000	50	3
21.45	0.0432	0.6480	50	35	57.16	0.0042	1.4000	50	3

### References

- Fig. 1.  $\sigma_{\text{tot}}$  cross-section of  $^{232}\text{Pa}$  between 0.12 MeV and 1.2 MeV. The data are plotted at intervals which correspond to a timing-channel width of 1.2 eV.
- Fig. 2.  $\sigma_{\text{tot}}$  cross-section of  $^{232}\text{Pa}$  between 0.1 and 0.2 MeV. The data are plotted at intervals which correspond to a timing-channel width of 1.2 eV except for the resonance at 177 keV where the channel width was kept at 0.5 eV. The error bars correspond to one standard deviation. For clarity, the data points at 177 keV are plotted with no error bars.
- Fig. 3.  $\sigma_{\text{tot}}$  cross-section of  $^{232}\text{Pa}$  multiplied by  $v^2/v_0^2$  between 0.4 eV and 1.0 eV. The averaged data correspond to a 24-ns channel width.

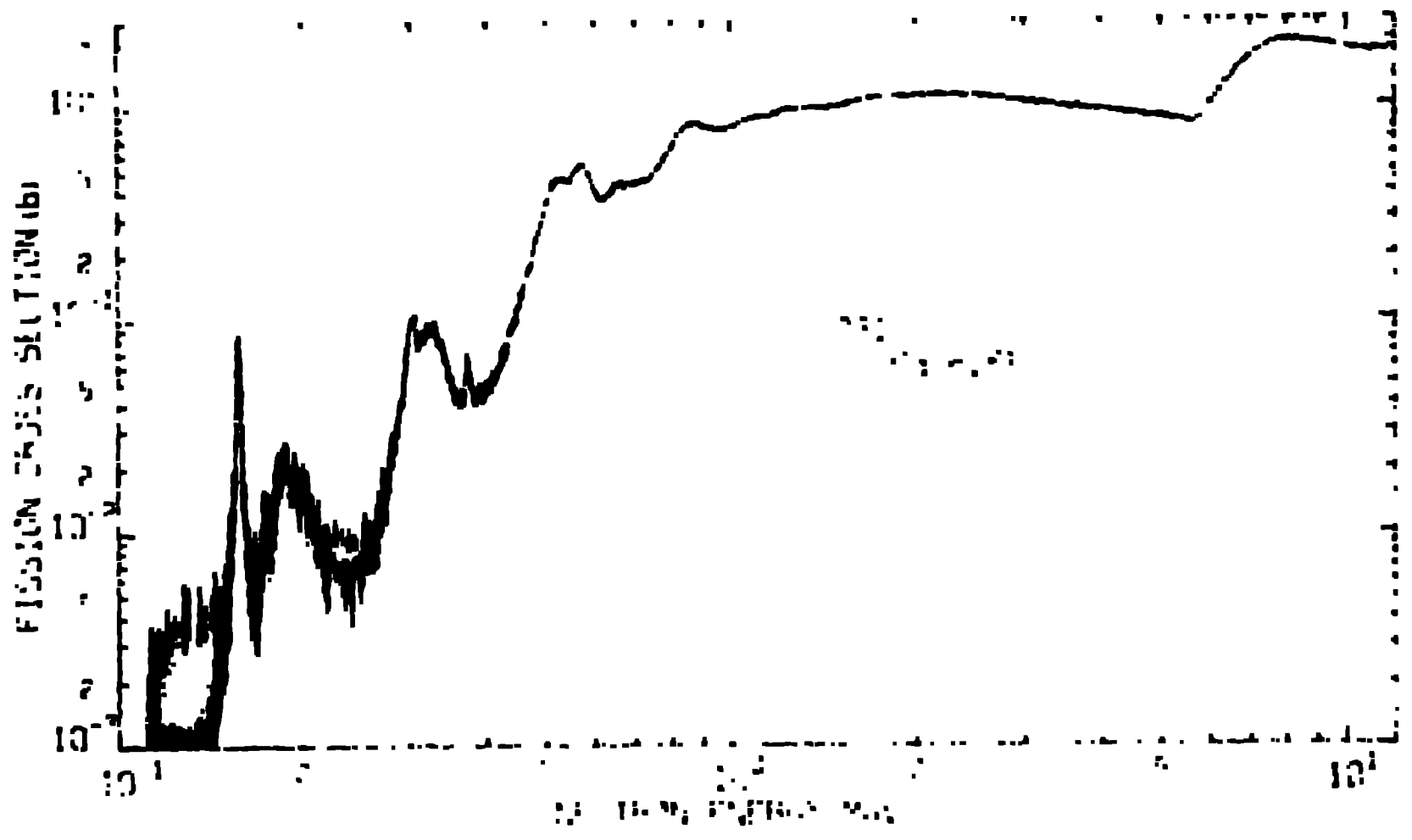


Figure 1.

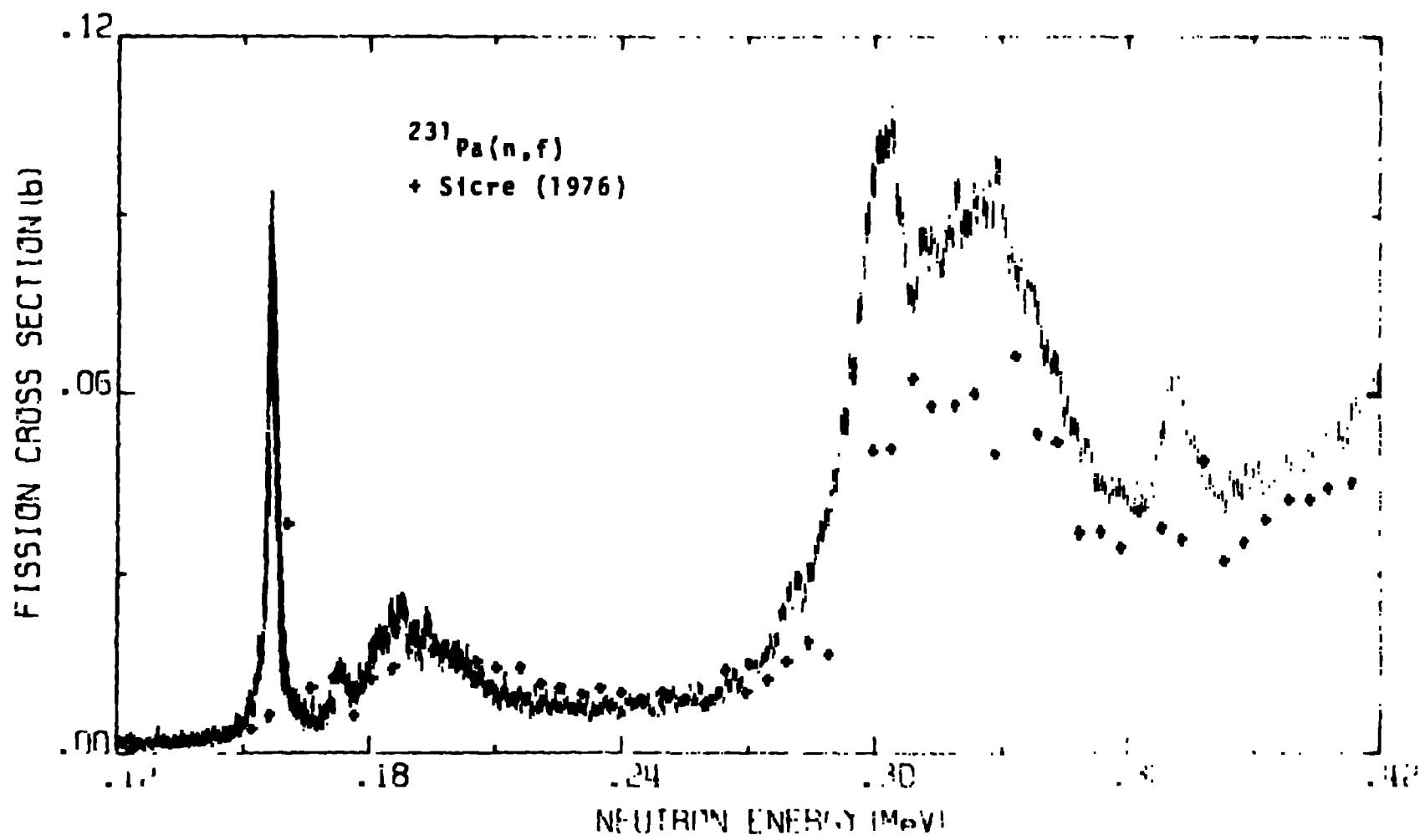


Figure 2.

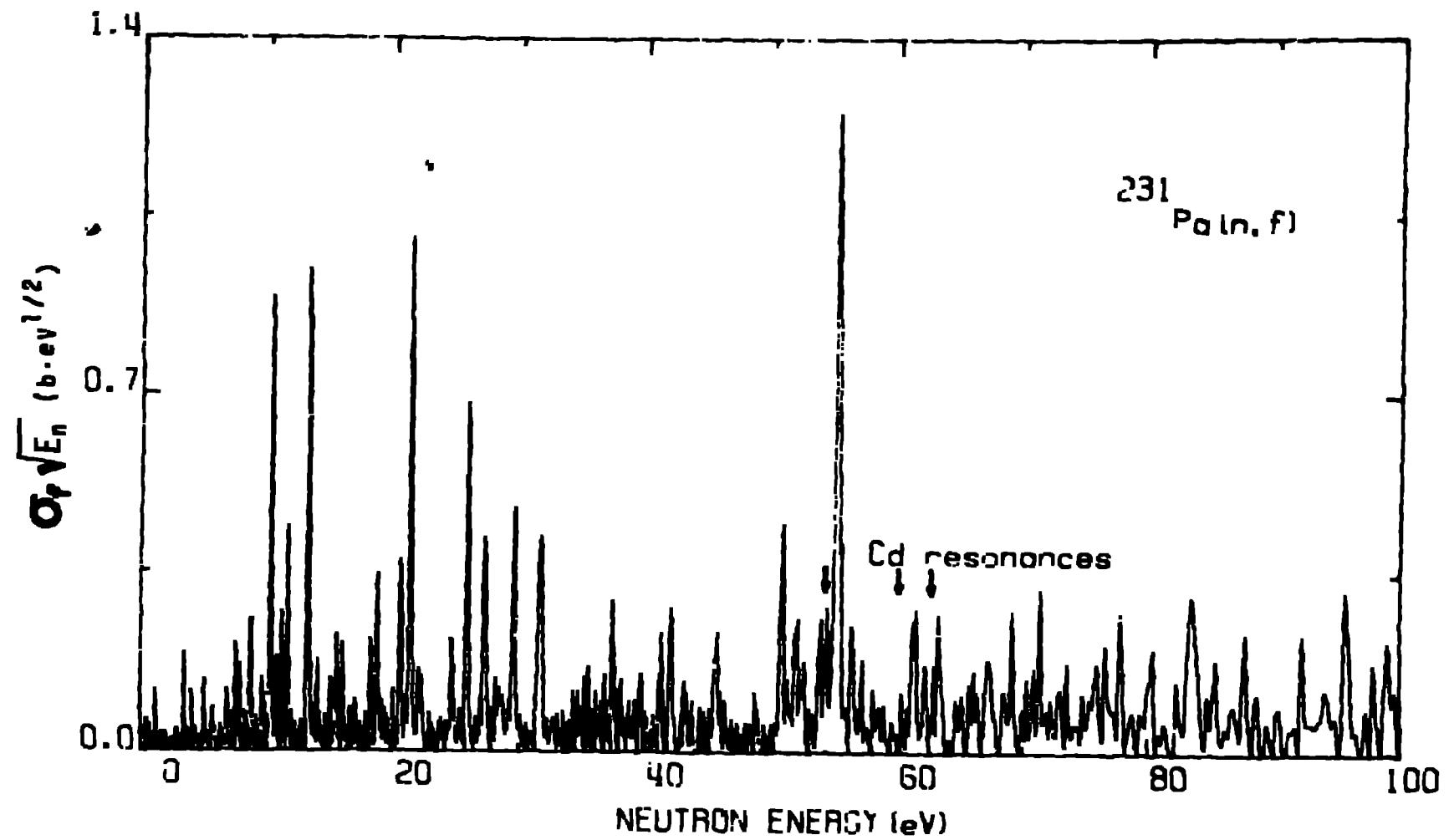


Figure 3.